Nonlocal and local equivalent microscopic optical potentials

W. Bauhoff,* H. V. von Geramb, and G. Pálla†
Theoretische Kernphysik, University of Hamburg, 2000 Hamburg 50, Federal Republic of Germany
(Received 16 February 1982)

Medium energy elastic proton scattering is analyzed with a microscopically generated nonlocal nucleon nucleus optical model. A thorough discussion is presented on the transition from a nonlocal potential to phase equivalent local potentials. These local potentials reveal a strong repulsive l-dependent core which is beyond phenomenological potential models. This core leads to a damping of the diffraction pattern at medium angles and a backward rise of the cross section. These features have been observed experimentally. The formalism is applied to scattering from ^{12}C and ^{40}Ca at low and medium energies and compared to experimental data.

[NUCLEAR REACTIONS Microscopic optical potential; $^{12}C(p,p)$, $E=40$, 180, 200 MeV; $^{40}Ca(p,p)$, $E=160$, 180 MeV; comparison with experimental data.]

I. INTRODUCTION

The theoretical study of elastic scattering processes in nuclear physics is a fundamental step in understanding the nuclear many body problem. Toward its solution the last three decades have put forward various approaches, lying between purely phenomenological and fully microscopic. Nucleon-nucleus scattering represents, thereby, the forefront of studies with more complex projectiles, and we consider the derivation of a complex single particle potential, the optical model potential (OMP), from the elementary nucleon-nucleon interaction as the ultimate goal.[1] The nuclear matter approach has been established as a qualitative and quantitative method of reconciling the success of the phenomenological local optical model potentials with a purely microscopic model.[2]

It is in the nature of the microscopic theory that various approximations are used, some of which are model truncations and some of which are solely computational conveniences. With the latter kind of approximations we refer to the solution techniques of the Bethe-Goldstone equation,[2,3] computations of the nonlocal folded OMP with nuclear matter t matrices, use of various forms for the diagonal and mixed single particle ground state density[4] and, what is our concern, the transition from nonlocal to local equivalent potentials.

In this paper we study problems and effects arising from the microscopic nonlocal OMP in differential cross section and polarization data. Closely connected with this aim is an investigation of local equivalent potentials in order to find differences with phenomenological OMP's. For a nonlocal operator one cannot tell if the interaction is purely attractive or purely repulsive simply by knowing the overall sign. One must consider the detailed structure of the nonlocality and its behavior as a function of energy and angular momentum. Some potentials are attractive at low energy and repulsive at high energy. Similarly, the behavior may change for different angular momenta and thus result in an effective l-dependent potential.

The investigation of Perey and Buck[5] for neutron scattering below 25 MeV with the Frahn and Lemmer[6] type of nonlocal potential is well known. The important result of this analysis was the reproduction of the energy dependence of local potentials with an energy-independent nonlocal potential and the reproduction of local phenomenological OMP's as equivalent potentials. Furthermore, the transition from nonlocal potentials to equivalent local potentials was achieved with successful approximate analytic expressions which have been little altered since.[7]

It has been pointed out by Austern[8] and later by Fiedeldey[9] and other authors[10] that nonlocal potentials are best elucidated by local equivalent potentials (LEQ) which are uniquely determined by a pair of linearly independent solutions of the nonlocal problem. An essential ingredient in this formulation is the damping of the nonlocal wave function as compared to the wave functions of the equivalent local potential. This effect, known as the Perey effect,[8,11] manifests an important difference between Schrödinger equations with a local and a nonlocal potential. A pair of linearly independent solutions

 ©1983 The American Physical Society

to local problems yields a constant Wronskian, independent of the radius. This radial independence of the Wronskian is generally not true for nonlocal potentials. This rigorous mathematical property makes it impossible to obtain identical solutions for local and nonlocal potentials without introducing singularities in the local potential.

In Sec. II we review the salient features of the microscopic nonlocal optical potential as it is generated from nuclear matter t matrices. This is understood as an example of a microscopic theory and it may be substituted by other approaches.[12,13] The definition of exact phase equivalent potentials in terms of nonlocal Wronskians and their derivatives is given in the following.

Section III contains the formulation of the LEQ when replacing the nonlocal Wronskian and its derivatives by pure properties of the nonlocal potential. The final result of this section is a series expansion for the LEQ. Several numerical examples are given to show qualitatively and quantitatively the differences with other methods of defining equivalent local potentials. An application with quantitative results for elastic proton scattering on ^{12}C and ^{40}Ca at various energies is given in Sec. IV. With these calculations we show the differences between phenomenological and microscopic optical potentials as they manifest themselves at low and high energies. The essential result shall be the occurrence of a repulsive core in the LEQ whose radius increases with angular momentum.

As compared to phenomenological potentials this establishes the importance of nonlocal potential analyses for scattering above 100 MeV. For lower energies we confirm that energy dependent and l-dependent potentials are sufficient to describe the global OMP. This is a numerical result independent of the existence of the repulsive core. For higher energies (around 200 MeV) consequences of the l-dependent potentials show up in the angular distribution which can be verified experimentally.

II. THEORETICAL BACKGROUND

The study of interacting nucleons in infinitely extended nuclear matter is well established, and approximate treatments for finite nuclei seem justified. Methods developed by Brueckner and Bethe have been widely applied and the theory is on firm ground[1-3] including calculational procedures for nucleon-nucleus elastic scattering starting from a realistic NN force.

The approach pursued in our studies is based on the evaluation of the effective internucleon t matrix from the free NN interaction.[3] The real and imaginary optical potential for nucleons is calculated to first order in the effective NN interaction with an improved version of the local density approximation (LDA) in a folding approach with single particle target densities. The model relies on the quite general approach to generating in first approximation the OMP as a sum of a direct term and a nonlocal exchange term:

$$u(\vec{r},\vec{r}';E)=\delta(\vec{r}-\vec{r}')\sum_n \int \phi_n^*(\vec{r}'')t_D(\vec{r},\vec{r}'';E)\phi_n(\vec{r}'')d^3r''+\sum_n \phi_n^*(\vec{r})t_E(\vec{r},\vec{r}';E)\phi_n(\vec{r}') \ . \tag{1}$$

The coordinates $\vec{r}$ and $\vec{r}'$ are projectile coordinates and the summation of single particle wave functions is used to represent the (Hartree-Fock) particle densities—diagonal and mixed—for protons and neutrons. The basic ingredient of the LDA enters here in the choice of t_D and t_E which are mixtures of direct and exchange effective NN interactions.[3] In principle it should be calculated in the finite system with its full structural details. We make the assumption that this effective interaction can be approximated locally by the interaction in nuclear matter for the same density and energy. This effective interaction is our version of LDA:

$$t_{D,E}(\vec{r},\vec{r}';E)=t_{D,E}\left[|\vec{r}-\vec{r}'|;k_F\left[\frac{\vec{r}+\vec{r}'}{2}\right],E\left[\frac{\vec{r}+\vec{r}'}{2}\right]\right] . \tag{2}$$

For brevity, the arguments of k_F and E will not be written in the following. The interaction contains automatically real and imaginary parts and the correct features of the finite range of the interaction. This is important since the ranges are different for real and imaginary parts and for the various spin and isospin channels. Any other approximation inherent in the nuclear matter approach in computing the effective interactions is not changed compared to previous calculations.[3]

The stationary Schrödinger equation

$$\Delta\psi(\vec{r},\vec{k})+[k^2-v_D(\vec{r})]\psi(\vec{r},\vec{k})=\int u(\vec{r},\vec{r}';E)\psi(\vec{r}',\vec{k})d\vec{r}' \tag{3}$$

for the single particle OMP scattering solutions is most easily solved in the standard partial wave decomposition, where the numerical problem is reduced to an ordinary second order integrodifferential equation, viz.,

$$\left[\frac{d^2}{dr^2}-\frac{L(L+1)}{r^2}+k^2-v_D(r)\right]\psi_{LJ}(r)=\int_0^\infty \omega_L(r,r')\psi_{LJ}(r')dr' \ . \tag{4}$$

The diagonal potential v_D contains the standard homogeneously charged sphere Coulomb potential. The spin orbit potential is obtained in a local form following Ref. 3 and is included in v_D as well. The multipole decomposition of the nonlocal OMP is formally obtained for a rotational invariant symmetric potential form,

$$u(\vec{r},\vec{r}')=u_D(r)\delta(\vec{r}-\vec{r}')+u_E(\vec{r},\vec{r}')=\sum_L \frac{\omega_L(r,r')}{rr'}[Y_L^*(\hat{r})\cdot Y_L(\hat{r}')]$$

$$=\sum_L \frac{(2L+1)}{4\pi}\omega_L(r,r')P_L(\hat{r}\cdot\hat{r}')/rr' \ . \tag{5}$$

The local direct potential is included in the exchange potential which represents the source of nonlocality. The energy dependence in (1) results from the small energy dependence of the effective interaction. The multipole decomposition, Eq. (5), is technically straightforward but is numerically quite involved due to required energy and density interpolation of numerically stored effective interactions.

The folding integral for the direct potential is simple and is generated with a Gauss-Legendre integration routine for the radial and angular integrations:

$$u_D(r)=2\pi\int_0^\infty dr''\int_{-1}^{1}dx\sum_{lj,\tau}S_{lj}^{\tau}t^D((r^2+r''2-2rr''x)^{1/2};k_F,E)\phi_{lj,\tau}{}^2(r'') \tag{6}$$

with S_{lj}^{τ} specifying the occupation number in the single particle orbit (lj) for protons/neutrons (τ). The radial wave functions $\phi_{lj,\tau}(r)$ are solutions of a Frahn-Lemmer type nonlocal bound state potential[14] with parameters $V_0=-72$ MeV, $R=1.2\,A^{1/3}$ fm, $a=0.65$ fm, and the range of nonlocality $\gamma=0.8$ fm including Coulomb and spin orbit potentials in the standard local form with $V_{ls}=7$ MeV, $R_{ls}=1.1\,A^{1/3}$ fm, $a_{ls}=0.65$ fm.

The exchange potential is directly generated in its multipole decomposition

$$u_E(\vec{r},\vec{r}')=\sum_{ST,n}\phi^*(\vec{r})\phi_n(\vec{r}')t_E^{ST}(\,|\,\vec{r}-\vec{r}'\,|\,;k_F,E)$$

$$=\frac{1}{rr'}\sum\phi_{lj,\tau}(r)\phi_{lj,\tau}(r')t_E^{ST}(\,|\,\vec{r}-\vec{r}'\,|\,;k_F,E)\mathscr{Y}_{lj,m}(\hat{r})\mathscr{Y}^*_{lj,m}(\hat{r}')S_{lj}^{\tau} \ . \tag{7}$$

In the limit of no-spin/isospin flip this expression assumes the form

$$u_E(\vec{r},\vec{r}')=\frac{1}{rr'}\sum\phi_{lj,\tau}(r)\phi_{lj,\tau}(r')S_{lj}^{\tau}\langle l\tfrac{1}{2}\mu\nu\,|\,jm\,\rangle^2$$

$$\times(-)^{S+T+1}\langle\tfrac{1}{2}\tfrac{1}{2}\nu\chi\,|\,Sm_s\,\rangle^2\langle\tfrac{1}{2}\tfrac{1}{2}\tau\epsilon\,|\,Tm_T\,\rangle^2 Y_{l\mu}(\hat{r})Y^*_{l\mu}(\hat{r}')t_E^{ST}(\,|\,\vec{r}-\vec{r}'\,|\,;k_F,E) \ . \tag{8}$$

Together with a multipole expansion of the effective interaction

$$t_E^{ST}(\,|\,\vec{r}-\vec{r}'\,|\,;k_F,E)=\sum t_\lambda^{ST}(r,r';k_F,E)[Y_\lambda^*(\hat{r})\cdot Y_\lambda(\hat{r}')] \ , \tag{9}$$

we obtain for the exchange contribution

$$\omega_L^E(r,r')=\sum_{\lambda lj,\tau}\phi_{lj,\tau}(r)\phi_{lj,\tau}(r')\langle l\lambda 00\,|\,L\,0\rangle^2 S_{lj}^{\tau}\frac{\hat{\lambda}}{2\pi\hat{L}}[\tfrac{1}{4}(t_\lambda^{01}-3t_\lambda^{11})\delta_{p\tau}+\tfrac{1}{8}(3t_\lambda^{10}+t_\lambda^{01}-t_\lambda^{00}-3t_\lambda^{11})(1-\delta_{p\tau})] \ . \tag{10}$$

The isospin (proton/neutron) of the projectile enters through the index p (for projectile) on the Kronecker symbol $\delta_{p\tau}$ and accounts for like or unlike projectile and target nucleons. As already mentioned, the required multipoles $t_\lambda^{ST}(r,r')$ are computed from tabulated values $t^{ST}(s;k_F,E)$. To eliminate possible errors in interpolations we apply a double Fourier-Bessel transformation and obtain

$$t_\lambda^{ST}(r,r';k_F,E)=8\int_0^\infty k\,dk\,j_\lambda(kr)j_\lambda(kr')\int_0^\infty s\,ds\,\sin(ks)t_E^{ST}(s;k_F,E) \ . \tag{11}$$

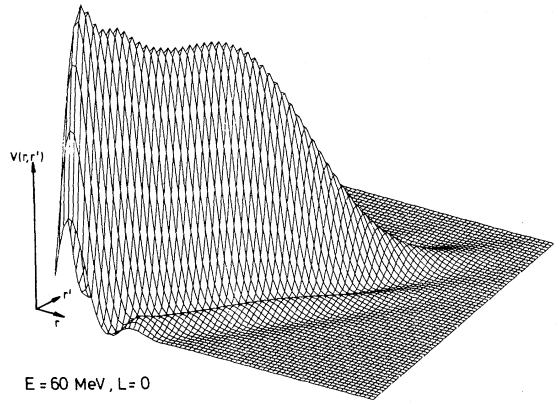

FIG. 1. Triaxial representation of the real nonlocal exchange kernel $\omega_0^E(r,r')$ for ^{40}Ca at 60 MeV.

An impression of the nonlocal exchange kernel is obtained from Figs. 1 and 2 where the radial dependence is shown for ^{40}Ca at 60 MeV for $L=0$ with cuts across the diagonal at $r+r'=6$ fm for several angular momenta. The multipole expansion of the local direct potential is straightforward and yields:

$$\omega_L^D(r,r')=u_D(r)\delta(r-r') \ . \tag{12}$$

With the generation of the nonlocal kernel for the central potentials and of the spin orbit potentials according to Ref. 3 all ingredients of Eq. (4) are available. It remains to solve the radial integrodifferential equation and extract the S-matrix elements in the usual matching procedure. Spurious states or bound states in the continuum are known to exist for some integrodifferential equations.[15] We defer further discussions of this problem since we checked our numerical results carefully and did not find any such case. With this comment we consider the problem solved, and the comparison of theoretical predictions with experimental data can be done.

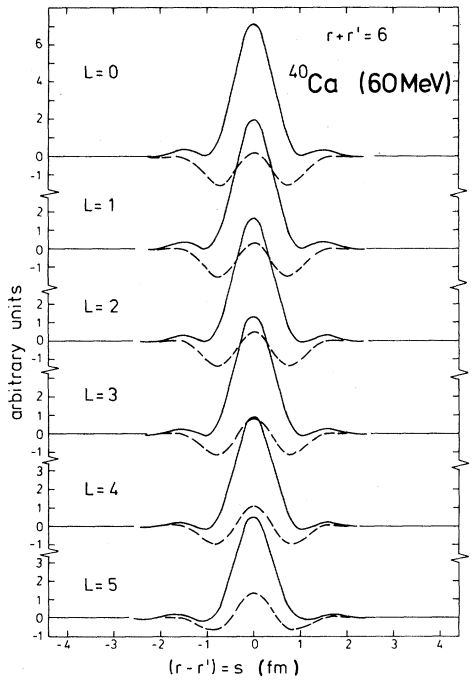

FIG. 2. Cuts of nonlocal exchange kernels $\omega_L^E(r,r')$ (real: solid lines, imaginary: dashed lines) for various angular momenta.

Since the standard phenomenological OMP analysis uses local potentials it appears desirable to construct a phase-equivalent local potential. We consider therefore the transformation of a Schrödinger equation with a nonlocal potential [Eq. (4)] to a Schrödinger equation with a local potential,

$$\left[\frac{d^2}{dr^2}-\frac{L(L+1)}{r^2}+k^2-v_D(r)\right]\psi_{LJ}(r) = V_{\rm eq}(r)\psi_{LJ}(r) \ . \tag{13}$$

The local potential $V_{\rm eq}(r)$ is said to be equivalent to the nonlocal kernel $\omega_L(r,r')$ if it can be completely specified in terms of Eq. (4) and its solutions and if it analytically reproduces all observable features for a fixed energy.

The transformation for the nonlocal equation requires two linearly independent solutions with asymptotically unique boundary conditions for incoming and outgoing waves.[9,10] The behavior in the interaction region may depend on assumptions about the interaction which are not subject to direct observation. The asymptotic properties are maintained in the transformation and are the same for both Eqs. (4) and (13). Let $f_{1,2}(k,r)$ be two solutions to the nonlocal radial equation and $F_{1,2}(k,r)$ the equivalent solutions to the local equation. Since $f_{1,2}$ and $F_{1,2}$ satisfy the same asymptotic boundary conditions, they are asymptotically equal,

$$\lim_{r->\infty}[f_i(k,r)-F_i(k,r)]=0 \ , \quad i=1,2 \ . \tag{14}$$

For finite distances we relate the solutions by a function $A(k,r)$:

$$f_i(k,r)=A(k,r)F_i(k,r) \ , \quad i=1,2 \tag{15}$$

which behaves asymptotically,

$$\lim_{r->\infty} A(k,r)=1 \ . \tag{16}$$

This ansatz was first suggested by Austern[8] and yields a smooth regular equivalent local potential. Any two linearly independent solutions define the Wronskian

$$W(f_1,f_2)=f_1(r)f_2'(r)-f_2(r)f_1'(r)\ . \tag{17}$$

This Wronskian shows the essential difference between local and nonlocal Schrödinger equations. Equation (17) is generally a function of the radius and is therefore different from $W(F_1,F_2)$, the local Wronskian, which is independent of the radius for regular potentials. Ansatz (15) together with (16) relates the Wronskian to the damping functions:

$$\begin{aligned} W(f_1,f_2)&=A^2(r)W(F_1,F_2)\\ &=A^2(r)W(F_1,F_2)\,|_{r=\infty}\\ &=A^2(r)W(f_1,f_2)\,|_{r=\infty}\ , \end{aligned} \tag{18}$$

so that the damping function is

$$A(k,r)=[W(f_1(k,r),f_2(k,r))/W(f_1(k,\infty),f_2(k,\infty))]^{1/2}\ . \tag{19}$$

The function $A(k,r)$ is in the literature often identified as the Perey effect[8,11] or damping function because it is usually smaller than 1.

The equivalent local potential is constructed in the same manner.[9,10] Combining Eqs. (4) and (13) we may eliminate any reference to a particular pair of solutions and find by pure algebraic manipulations that

$$\begin{aligned} V_{\rm eq}(r)&=-\frac{1}{2}\frac{W''(f_1,f_2)}{W(f_1,f_2)}+\frac{3}{4}\left[\frac{W'(f_1,f_2)}{W(f_1,f_2)}\right]^2\\ &\quad+\frac{1}{W(f_1,f_2)}\cdot\int_0^\infty \omega_L(r,r')[f_1(r')f_2'(r)-f_1'(r)f_2(r')]dr'\\ &=-\frac{A''}{A}+2\left[\frac{A'}{A}\right]^2+\frac{1}{A^2}\int_0^\infty \omega_L(r,r')[f_1(r')f_2'(r)-f_2(r')f_1'(r)]dr'\ . \end{aligned} \tag{20}$$

The expressions for the damping function and equivalent local potential provide mathematically rigorous definitions of these l-dependent quantities for the full radial range. So we have a method to compare microscopic l-dependent potentials with the usual phenomenological potentials.

The transition from the nonlocal potential to a phase-equivalent local one is certainly not unique. We have fixed the local potential by requiring the same damping function $A(k,r)$ for any solution of the Schrödinger equation. It is possible to relax this condition and allow for different damping functions for different solutions.[16] Furthermore, it is possible to replace the local damping function $A(k,r)$ by an integral kernel relating local and nonlocal solutions which is asymptotically equal to a δ function. The prescription we have adopted is the most simple one and is the only one which has been used in actual calculations before.[10] It must be kept in mind, however, that all observables calculated from any local phase-equivalent potential will be identical because they reflect only the properties of the original nonlocal kernel. So an enhancement of the cross section at backward angles, e.g., will be found for any phase-equivalent potential if it is found for one, irrespective of the form of the particular potential.

It is of some interest to discuss properties of the above defined damping function and equivalent local potential for $r\to 0$. In general, we have

$$\begin{aligned} W'(r)=\int_0^\infty \omega_L(r,r')[&f_1(r)f_2(r')\\ &-f_1(r')f_2(r)]dr'\ . \end{aligned} \tag{21}$$

For symmetric kernels

$$\omega_L(r,r')=\omega_L(r',r)$$

it follows

$$W(\infty)-W(0)=\int_0^\infty W'(r)dr=\int_0^\infty \omega_L(r,r')[f_1(r)f_2(r')-f_1(r)f_2(r')]dr\,dr'=0\ , \tag{22}$$

so that for the damping function we have

$$\lim_{r\to 0} A(k,r)=1\ .$$

It does not seem to be possible to give a simple expression for $V_{\rm eq}(0)$. Since our kernels result from a multipole decomposition they behave close to the origin like

$$\lim_{r,r'\to 0}\omega_L(r,r')=\frac{r^{L+1}r'^{L+1}}{\text{const}}\ . \tag{23}$$

For such a kernel,

$$\lim_{r\to 0} W'(r)=0$$

as can be seen from Eq. (21) together with the well-

known behavior of regular and irregular solutions at the origin. Furthermore, the third term in Eq. (20) vanishes at $r=0$ for $L=0$ (but not for $L\neq 0$) since in this case regular and irregular solutions have zero slope at the origin. So we have a contribution for $r=0$, $L=0$ only from the term involving W''. If we assume that the damping function $A(k,r)<1$ for $r\neq 0$ (this is found in all calculations up to now,[8–10] but we do not have a general proof for it), then $W''(0)<0$ and $V_{\rm eq}(0)>0$ for $L=0$ even if $\omega_L(r,r')<0$ for all r,r'. This peculiar behavior reflects the form of the integral kernel on the boundaries $r,r'=0$ [Eq. (23)]. For a nonvanishing nonlocality range γ the integral kernel $\omega_L(r,r')$ vanishes at $r=r'=0$, but becomes increasingly steep for $\gamma\to 0$. In the limit $\gamma=0$ we have a local potential with a finite (negative) value at $r=0$.

III. ANALYTIC REPRESENTATION OF THE LOCAL l-DEPENDENT POTENTIALS

Although Eq. (20) gives an exact expression for the local equivalent potential, it is quite cumbersome to use in practice since two independent solutions are needed for the calculation. Therefore, it seems desirable to develop an approximation scheme for the calculation of $V_{\rm eq}(r)$. The quality of the approximation can then be tested by comparison with the exact formula (20). Such a comparison was not possible for other approximations[7–9] which do not make use of an angular momentum decomposition. The basic idea of the approximation scheme is to use a perturbation expansion with respect to the nonlocality range of the integral kernel. For any symmetric integral kernel $\omega(r,r')$ the following equality can be proven:

$$\omega(r,r')=\sum_{n=0}^{\infty}\frac{(-1)^n}{n!}e^{ik_0(r-r')}\times\delta^{(n)}(r-r')v_n\left[\frac{r+r'}{2};k_0\right], \quad (24)$$

where

$$k_0=k_0\left[\frac{r+r'}{2}\right]$$

is an arbitrary function to be chosen later and the expansion coefficients v_n are determined by the following equation [$s=r-r'$, $R=\frac{1}{2}(r+r')$]:

$$v_n(R;k_0)=\int_{-2R}^{2R}e^{-ik_0 s}s^n\omega(R+\tfrac{1}{2}s,\,R-\tfrac{1}{2}s)ds\ . \quad (25)$$

A formal proof for this equality is obtained by inserting the expansion (24) under the integral in (25):

$$v_n(R;k_0)=\int_{-2R}^{2R}ds\,s^n\sum_{m=0}^{\infty}\frac{(-1)^m}{m!}\delta^{(m)}(s)v_m(R;k_0)\ . \quad (26)$$

All terms of the sum drop out by m-fold partial integration except $m=n$; so the proof results.

v_n is the nth moment of the integral kernel $\omega(r,r')$. The approximation scheme to be described may therefore be called a moment expansion. For the special case $k_0(r)\equiv 0$ this type of expansion has been used in the framework of generator coordinate theory.[17] Since in our case the arguments of $\omega(r,r')$ are restricted to positive values the integration with respect to $s=r-r'$ is on a finite interval only. It is now important to note that the moments $v_n(R;k_0)$ will decrease rather rapidly with increasing n due to the peculiar form of the integral kernel. Since $\omega(r,r')$ is strongly peaked at $s=r-r'=0$ (see Fig. 1), an appreciable contribution to the integral (25) comes only from the region of small s. The factor s^n, however, is small there for $n>0$, so the value of the whole integral will decrease with increasing n. From this consideration, it is suggestive to consider (24) as a perturbation expansion of the integral kernel. This can be seen explicitly if $\omega(r,r')$ has a Gaussian nonlocality with range γ. Then v_n will be proportional to γ^n, so we have an expansion with respect to the nonlocality. In the general case a parameter λ will be introduced to characterize the magnitude of the various orders so that Eq. (24) can be written

$$\omega(r,r')=\sum_{n=0}^{\infty}\lambda^n V_n(r,r';k_0) \quad (27a)$$

with

$$V_n(r,r';k_0)=\frac{(-1)^n}{n!}e^{ik_0(r-r')}\times\delta^{(n)}(r-r')v_n\left[\frac{r+r'}{2};k_0\right]. \quad (27b)$$

If this expansion is introduced into the nonlocal Schrödinger equation, a corresponding expansion for the wave function is appropriate:

$$f(r)=\sum_n\lambda^n f_n(r)\ . \quad (28)$$

Equating now equal powers of λ on both sides, the nonlocal Schrödinger equation is transformed into a set of local equations. The lowest order equations read, explicitly,

$$\left[\frac{d^2}{dr^2}-\frac{L(L+1)}{r^2}+k^2-v_0(r)\right]f_0(r)=0\ ,$$
$$\left[\frac{d^2}{dr^2}-\frac{L(L+1)}{r^2}+k^2-v_0(r)\right]f_1(r)=\int V_1(r,r';k_0)f_0(r')dr'\ , \tag{29}$$
$$\left[\frac{d^2}{dr^2}-\frac{L(L+1)}{r^2}+k^2-v_0(r)\right]f_2(r)=\int V_1(r,r';k_0)f_1(r')dr'+\int V_2(r,r';k_0)f_0(r')dr'\ .$$

So the zeroth order equation is a standard local Schrödinger equation whereas all higher equations contain an inhomogeneous term, which is determined by the solutions of the lower equations. As $V_n(r,r';k_0)$ contains derivatives of the δ function, the inhomogeneities are in fact local expressions containing derivatives of the wave functions. Second and higher derivatives of them may be eliminated by using the lower order equations.

If two independent solutions $f(r),g(r)$ are expanded in the form (28), a corresponding expansion will result also for the Wronskian $W(r)$ which reads, explicitly up to order λ,

$$\begin{aligned}W(r)&=W_0(r)+\lambda W_1(r)+\cdots\\&=[g_0(r)f_0'(r)-g_0'(r)f_0(r)]\\&\quad+\lambda[g_0(r)f_1'(r)+g_1(r)f_0'(r)\\&\qquad-g_0'(r)f_1(r)-g_1'(r)f_0(r)]\\&\qquad+\cdots\ .\end{aligned}\tag{30}$$

From the set of equations (29) it is, however, seen that $W_0(r)$ is a Wronskian corresponding to a usual local Schrödinger equation. It is well known that in this case the Wronskian does not depend on the radius, so we have the important result:

$$W_0(r)=W_0(\infty)=\text{const}\ . \tag{31}$$

After these preliminaries we return to the question of approximating the phase equivalent potential $V_{\text{eq}}(r)$, Eq. (20). From the expansion in powers of λ for the integral kernel and the Wronskian we will get also an expansion for $V_{\text{eq}}(r)$. It will be shown that the various contributions can be calculated from the knowledge of the moments of the integral kernel and that any wave function drops out of the final formula. The full calculation is rather lengthy, so we will consider only a single term to demonstrate the method. As an example take the term

$$\left[\frac{W'(r)}{W(r)}\right]^2\ .$$

From (30) we have

$$W'(r)=W_0'(r)+\lambda W_1'(r)+\cdots\ . \tag{32}$$

The first term on the right-hand side vanishes due to Eq. (31). Up to order λ we have

$$\frac{W'(r)}{W(r)}=\frac{W_1'(r)}{W_0(\infty)}\ . \tag{33}$$

With the definition (30) we find, for the derivative,

$$\begin{aligned}W_1'(r)&=f_0''(r)g_1(r)+f_1''(r)g_0(r)\\&\quad-f_0(r)g_1''(r)-f_1(r)g_0''(r)\ .\end{aligned}\tag{34}$$

The second derivatives of the wave functions may now be eliminated with help of the Schrödinger equations (29). Many terms cancel, and we have remaining

$$\begin{aligned}W'(r)&=g_0(r)\int V_1(r,r';k_0)f_0(r')dr'\\&\quad-f_0(r)\int V_1(r,r';k_0)g_0(r')dr'\ .\end{aligned}\tag{35}$$

Finally, we use the definition (27b) for $V_1(r,r';k_0)$ to obtain

$$W_1'(r)=v_1(r;k_0)[g_0(r)f_0'(r)-f_0'(r)g_0(r)]\ . \tag{36}$$

The expression in square brackets is

$$W_0(r)=W_0(\infty)\ .$$

$W_0(\infty)$ cancels in Eq. (33) and we get as a contribution to the potential $V_{\text{eq}}(r)$ from the term

$$\left[\frac{W'(r)}{W(r)}\right]^2\ ,$$

up to order λ^2,

$$\left[\frac{W'(r)}{W(r)}\right]^2=\lambda^2 v_1^2(r;k_0)\ . \tag{37}$$

As claimed at the beginning, this expression does not contain the wave function anymore, but only the (first) moment of the integral kernel. Similarly, all other contributions to the phase equivalent potential can be calculated. The final result up to order λ^2 reads

$$V_{\rm eq}(r)=v_0(r;k_0)+\lambda[-ik_0v_1(r;k_0)]+\lambda^2\left[\tfrac{1}{4}v_1{}^2(r;k_0)-\tfrac{1}{4}v_2''(r;k_0)\right.$$

$$\left.+v_2(r;k_0)\left[\frac{L(L+1)}{r^2}-k^2+v_0(r;k_0)-k_0{}^2\right]\right]. \tag{38}$$

Of course, $\lambda=1$ in the final expression. The inclusion of higher order terms does not present essential difficulties but the calculations become rather lengthy.

This expression for $V_{\rm eq}(r)$ may be transformed further by elimination of all odd moments. For a symmetric integral kernel $\omega(r,r')$ we have, explicitly,

$$v_1(R;k_0)=i\int_{-2R}^{2R} s\sin k_0s\,\omega(R-\tfrac{1}{2}s,\ R+\tfrac{1}{2}s)ds\ . \tag{39}$$

Since only the region around $s=0$ is important in the integral we can expand $\sin k_0s$ around $s=0$ in the form

$$\sin k_0s=k_0s-\tfrac{1}{6}k_0{}^3s^3+\cdots\ . \tag{40}$$

This expansion relates v_1 to v_2 and higher even moments:

$$v_1(r;k_0)=2ik_0v_2(r;k_0)+8ik_0{}^3v_4(r_0;k_0)+\cdots\ . \tag{41}$$

Similarly, v_3 and higher odd moments can be eliminated. If this expression is substituted into Eq. (38), we get ($\lambda=1$)

$$V_{\rm eq}(r)=v_0(r;k_0)-\tfrac{1}{4}v_2''(r;k_0)+v_2(r;k_0)\left[\frac{L(L+1)}{r^2}-k^2+v_0(r;k_0)+k_0{}^2\right]. \tag{42}$$

If the whole series is summed, the result does not depend on the choice of $k_0(r)$. It is, however, important to choose it in an appropriate way, if only a few terms are taken into account. By comparing the exact potential Eq. (20) with the partial sum of the moment expansion it is possible to see whether the particular choice of $k_0(r)$ is a good one or not. It turns out that the agreement between the exact potential and the zeroth order of the moment expansion is closest when $k_0(r)$ is chosen self-consistently[7] as the local momentum of the projectile,

$$k_0{}^2(r)=k^2-\frac{L(L+1)}{r^2}-v_0(r;k_0)\ . \tag{43}$$

The reason for this agreement can be seen by inspecting Eq. (42). For this choice of $k_0(r)$, the last term drops out and the only correction to v_0 is v_2'' which is very small. Inside nuclear matter, the potential does not depend on the position, so in this case the second order correction vanishes completely for the self-consistent choice of $k_0(r)$. So in lowest order, the phase equivalent potential is given by

$$V_{\rm eq}(r)=v_0(r;k_0)=\int_{-2r}^{2r} e^{-ik_0(r)s}\times\omega_0(r+\tfrac{1}{2}s,\ r-\tfrac{1}{2}s)ds \tag{44}$$

with $k_0(r)$ given by (43). For $L\neq0$ and r sufficiently small, $k_0{}^2$ will become negative and hence k_0 imaginary. Since only even powers of k_0 occur in the calculation of $V_{\rm eq}$ for a symmetric integral kernel $\omega(r,r')$, $V_{\rm eq}$ will stay real. Another possible choice for k_0 would be $k_0=0$ when the right-hand side of Eq. (43) is negative. Explicit calculations have shown that the approximate local potential with this form of k_0 does not reproduce the exact local potential given by Eq. (20) as closely as for the self-consistent value of k_0. So we require self-consistency also for negative $k_0{}^2$. All results presented in the following are obtained with this special $k_0(r)$.

From its definition it is seen that $v_0(0)=0$ for a nonsingular kernel whereas the exact $V_{\rm eq}$ does not vanish at the origin. The error in calculating the phase shifts caused by this discrepancy is negligible for the microscopic optical potentials for two reasons. First, due to the absorption the wave function is strongly damped in the nuclear interior so that the value of the potential close to the origin has little influence on the cross section. Second, the strongly repulsive direct potential determines the behavior at the origin so that only a small error in a small contribution to the complete result arises.

The first term of the moment expansion is similar to the first term of the expansion proposed by Perey and Saxon[7] if their expansion is applied to the kernel decomposed into multipoles. It differs only in the

integration range and is identical to the Perey-Saxon approximation for radii larger than the nonlocality range. In higher orders, the moment expansion is conceptually different since it only introduces corrections to the potential but does not lead to second or higher order differential operators. For all energies considered the zeroth order of the moment expansion has been found to be sufficiently accurate. Therefore, we have kept only this term in the calculations. We have not investigated whether this is a valid approximation for larger nonlocalities. From the nature of the expansion it is clear that the truncation of the series after the first term is justified for all smaller nonlocalities.

In order to compare the various approaches for a phase equivalent local potential we consider first a model of simple analytic form, the so-called Frahn-Lemmer[6] or Perey-Buck[5] potential, which is given by

$$u(\vec{r},\vec{r}')=\frac{V_0}{\gamma^3\pi^{3/2}}e^{-(\vec{r}-\vec{r}')^2/\gamma^2}\left\{1+\exp\left[\frac{1}{a}\left[\frac{r+r'}{2}-R\right]\right]\right\}^{-1}. \tag{45}$$

Its various multipole components can be calculated analytically.[5] The parameters have been chosen for ^{40}Ca, i.e., $R=4.1$ fm, $a=0.65$ fm. The depth is taken as $V_0=-72$ MeV, and the nonlocality range is $\gamma=0.8$ fm. Various forms of the equivalent local potential[5] are shown in Fig. 3 for the s wave at a projectile energy of 30 MeV. First of all, the trivially equivalent potential has so many singularities that a smooth interpolation seems rather arbitrary. The phase-equivalent potential Eq. (20) has a conventional Woods-Saxon shape at larger radii, but deviates from this form strongly at small distances. For $r\to 0$ it is even repulsive. This has to be expected from the general discussion in Sec. II. The potential

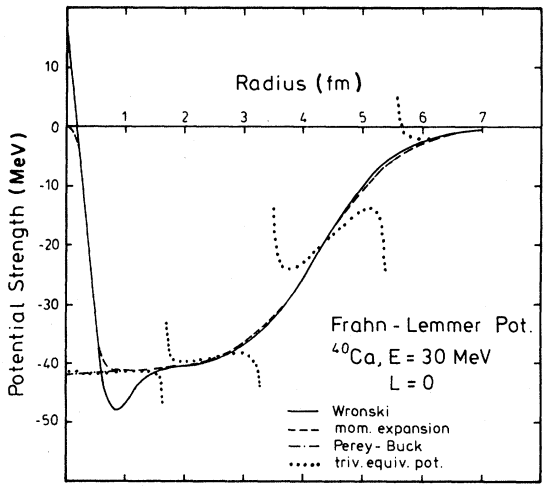

FIG. 3. Comparison of equivalent local potentials, generated with different prescriptions. The Wronski method (solid line) is the exact result for Eq. (20), and moment expansion refers to Eq. (37). The Perey-Buck potential and trivial equivalent potentials coincide with its definition in Ref. 5.

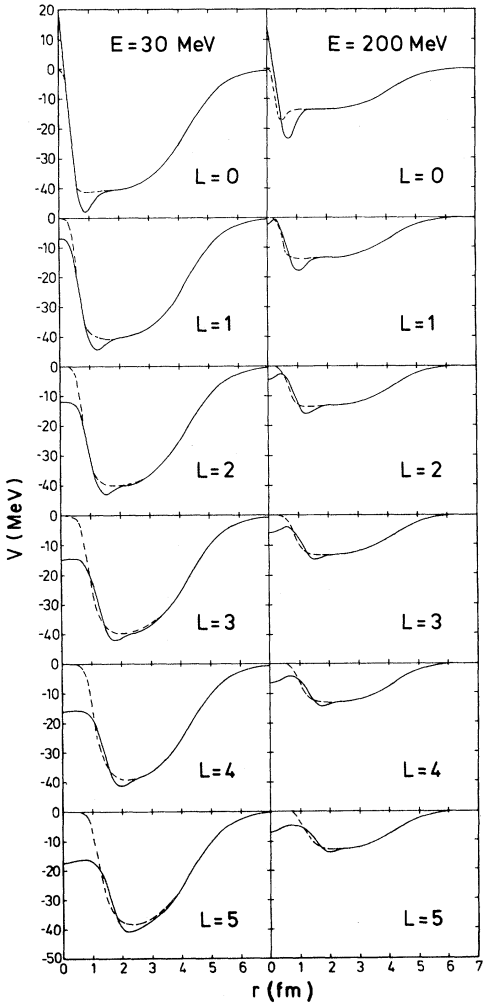

FIG. 4. Comparison of the phase-equivalent local potentials calculated with the Wronski method (solid line) and with the moment expansion (dashed line) for two energies and various angular momenta.

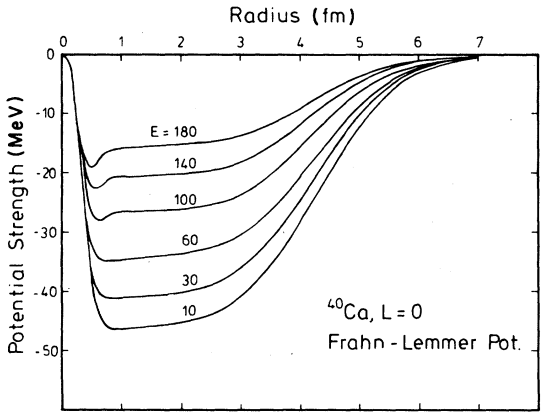

FIG. 5. Energy dependence of the local equivalent Frahn-Lemmer type potential generated with moment expansion.

resulting from the moment expansion deviates only slightly from this form: it does not show the dip around 1 fm, and it vanishes at the origin. For comparison, also the usual Perey-Buck approximation is shown which does not depend on the angular momentum. It coincides with the moment expansion everywhere except close to the origin where it has a finite negative value.

The accuracy of the exactly phase equivalent potentials can be checked rather easily. If two linearly independent solutions are obtained for the intergrodifferential equation, the local potential and the Perey effect can be computed. Then two solutions to the local problem are calculated and compared to the nonlocal wave functions which were multiplied by the Perey effect. Any difference between these results is due to numerical inaccuracies. The potentials calculated with the moment expansion are compared with the exact ones in Fig. 4 for two energies

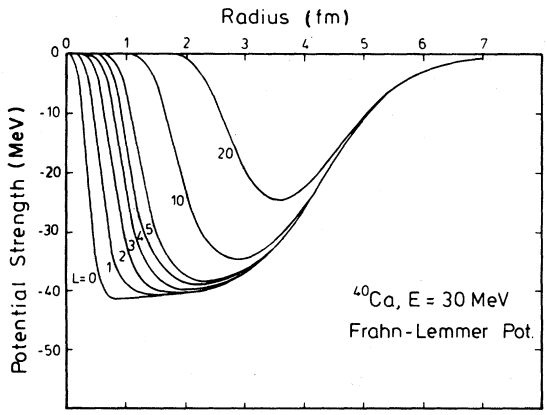

FIG. 6. Study of the l dependence of the equivalent Frahn-Lemmer potential for 30 MeV nucleons.

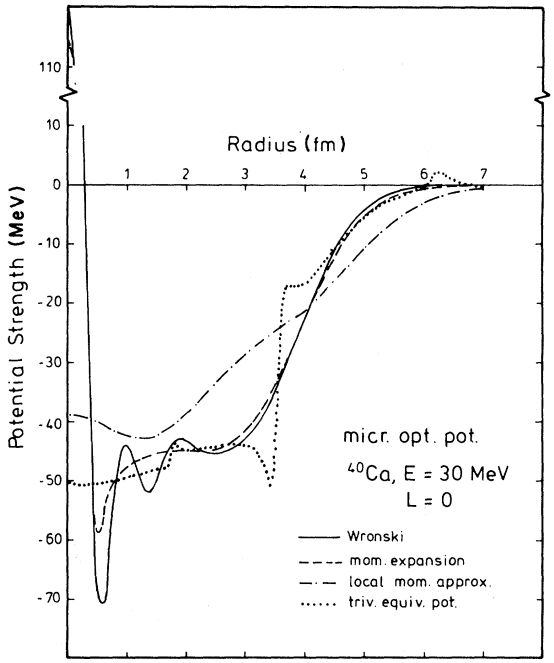

FIG. 7. Comparison of various equivalent local potentials when applied to the full microscopic optical model kernel. Wronski refers to the exact solution of Eq. (20) and moment expansion to Eq. (37). The local momentum approximation has been used in Ref. 3. Trivial equivalent is identical with Ref. 5.

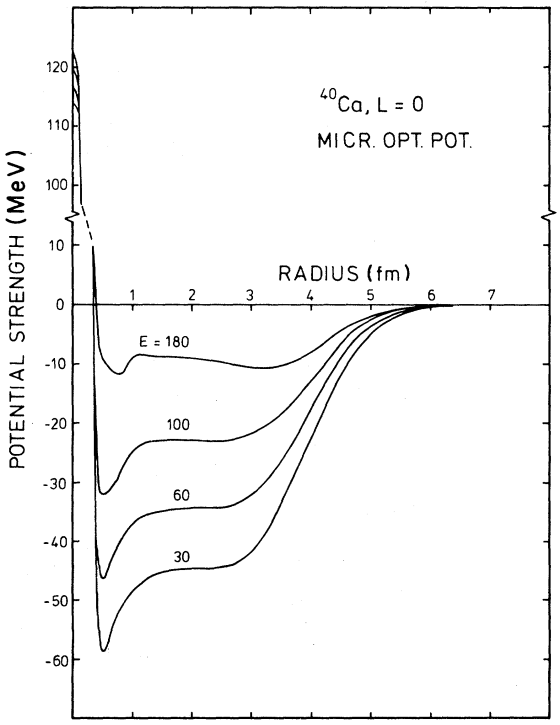

FIG. 8. Study of the energy dependence of the real part of LEQ within the moment expansion.

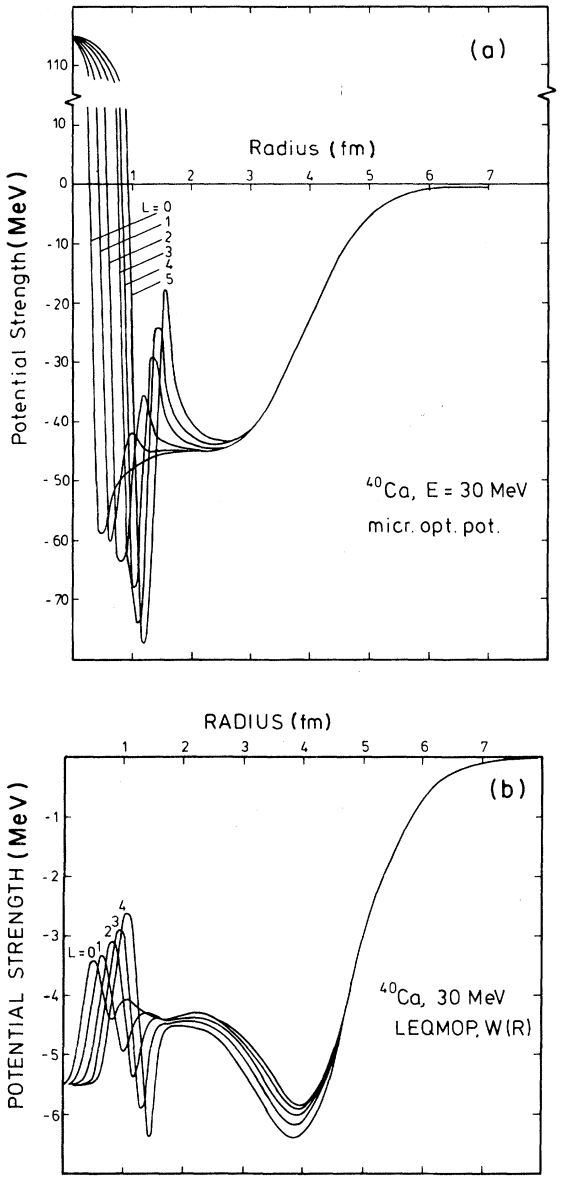

FIG. 9. (a) l dependence of the real part of LEQ within the moment expansion. (b) l dependence of the imaginary part of LEQ within the moment expansion.

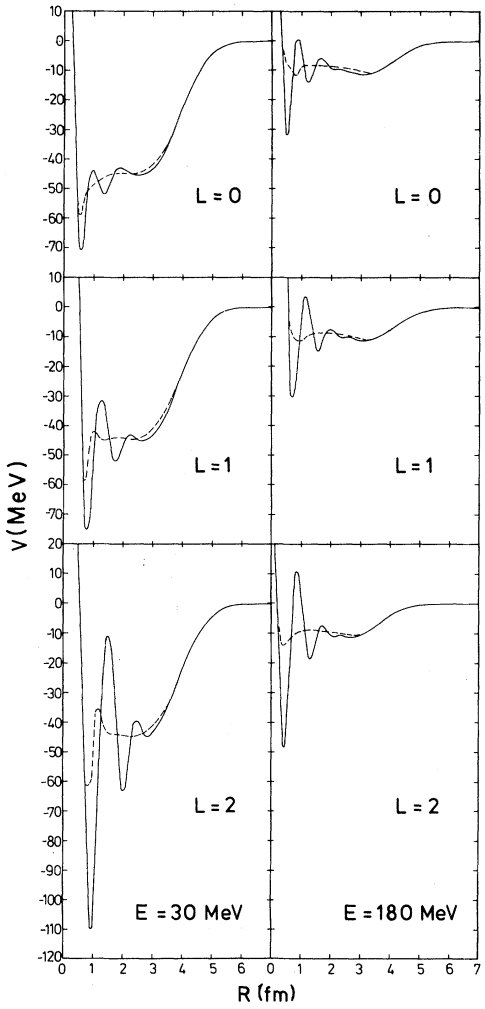

FIG. 10. Comparison of the potentials calculated with the Wronski method (solid line) and with the moment expansion (dashed line) for the real part of the microscopic optical potential.

and angular momenta up to $L=5$. For still higher angular momenta the exact formula Eq. (20) leads to numerical difficulties. The agreement between exact and approximate potentials is very good. A notable difference is found only for very small distances where the approximate potential approaches zero in contrast to the exact one. This discrepancy affects only the large angle cross section which will be overestimated by the moment expansion.

In Fig. 5, we consider the energy dependence of the local potential resulting from the moment expansion. The behavior at short distances is found to be independent of the energy whereas for larger distances the potential decreases almost linearly with the energy. The behavior for different angular momenta at the same energy, shown in Fig. 6, is complementary to this. For large distances, the potential does not depend on L, whereas the short-distance behavior is completely different for different angular momenta. The potential can be shown to start like r^{2L+3}.

The corresponding results for the real part of the microscopic optical potential are shown in Figs. 7 to 10. In this case one has to add a local (repulsive) potential to the nonlocal attractive one. Therefore, the

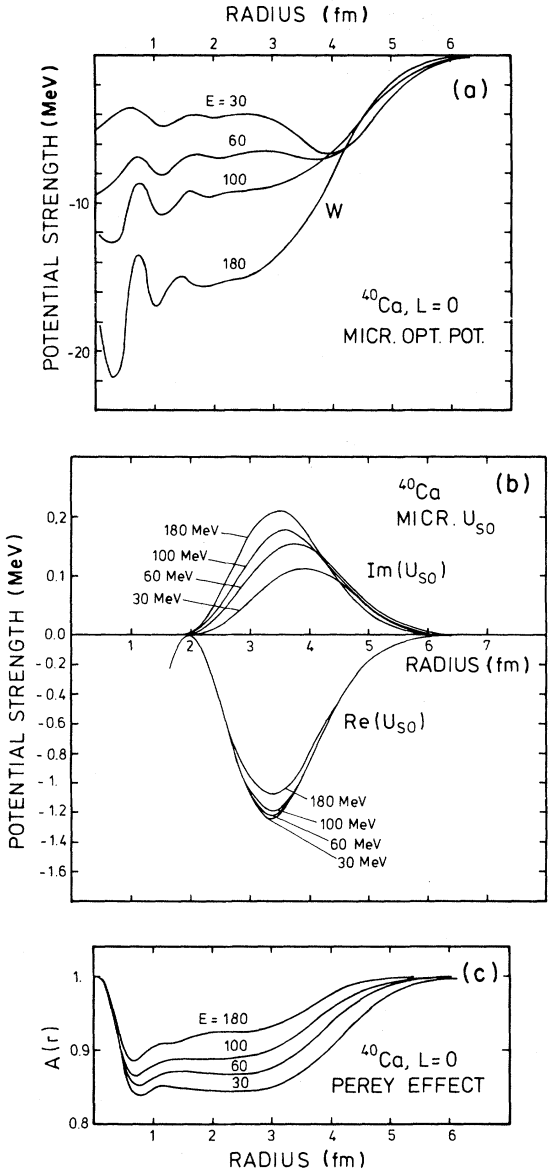

FIG. 11. (a) Energy dependence of full imaginary central potential. (b) Local spin orbit potentials generated according to Ref. 3. Note the different scale for real and imaginary parts. (c) Energy dependence of the real part of the damping function (Perey effect) for $L=0$ based on the full nonlocal kernel.

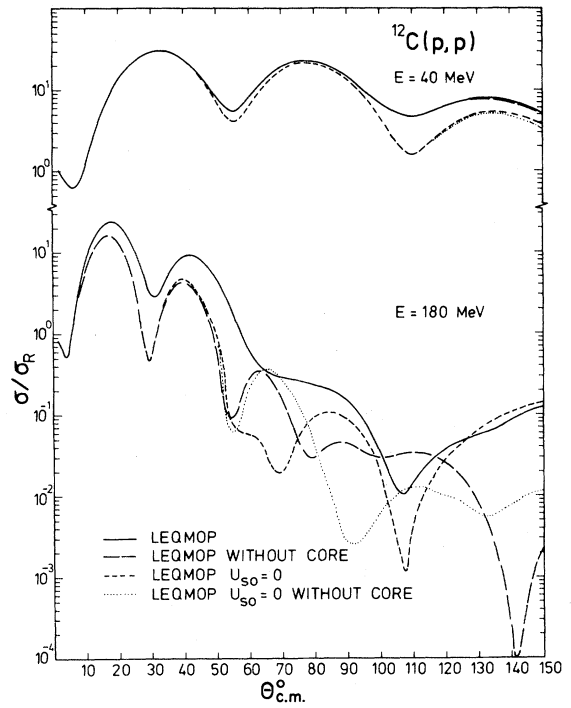

FIG. 12. Effects of the repulsive l-dependent core on differential cross sections at low and medium energy. The geometry is for ^{12}C.

behavior close to the origin is dominated by the direct term which leads to the existence of a repulsive core. The various equivalent local potentials are compared in Fig. 6. The trivially equivalent potential does not have singularities because the wave function is now complex. Instead it shows finite jumps at the zeros of the real part of the wave function. The exact potential has various oscillations for small distances which are interpolated by the moment expansion. Such a smoothing behavior had to be expected since the zeroth order moment is essentially given by the Wigner transform of the nonlocal potential which cannot reproduce all quantum fluctuations. The local momentum approximation used by Brieva and Rook[3] is seen to differ strongly for all radii, so this approximation seems to be questionable.

The energy dependence of the local potential (Fig. 8) is similar to that obtained for the Frahn-Lemmer potential. Much more interesting is the angular momentum dependence shown in Fig. 9. One observes the existence of a pronounced oscillation between 1 and 2 fm which is amplified for larger angular momenta.

For such an oscillatory potential one may question the validity of the moment expansion. It is therefore compared to the exact results of the Wronski method in Fig. 10. The exact potentials show even larger oscillations than the approximate ones. So the appearance of the oscillations is not a consequence of the moment expansion and, in particular, not of the occurrence of negative values of k_0^2 for $L\neq 0$. If analyzed in more detail, the angular momentum dependence is found to be roughly of the

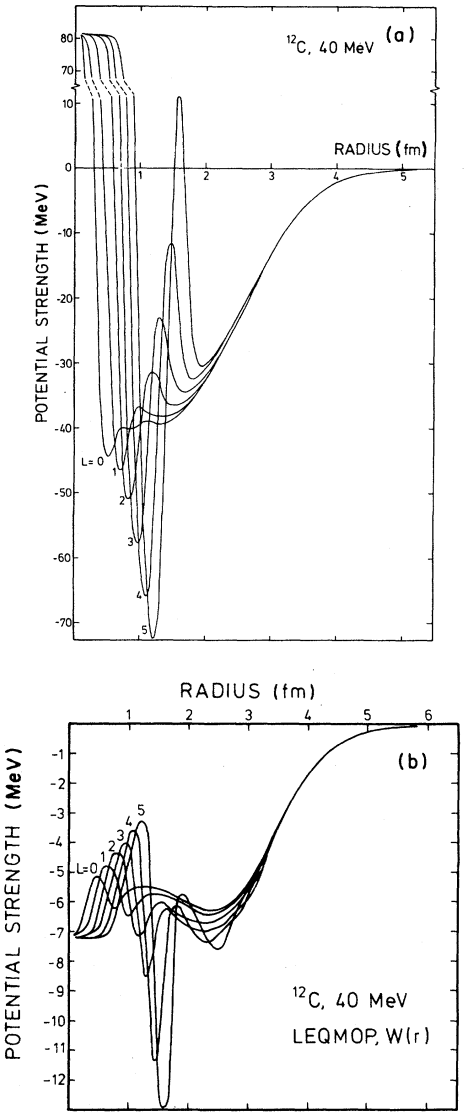

FIG. 13. (a) 40 MeV l-dependent real central potentials underlying the calculations in Fig. 12. (b) 40 MeV l-dependent imaginary central potentials underlying the calculations in Fig. 12.

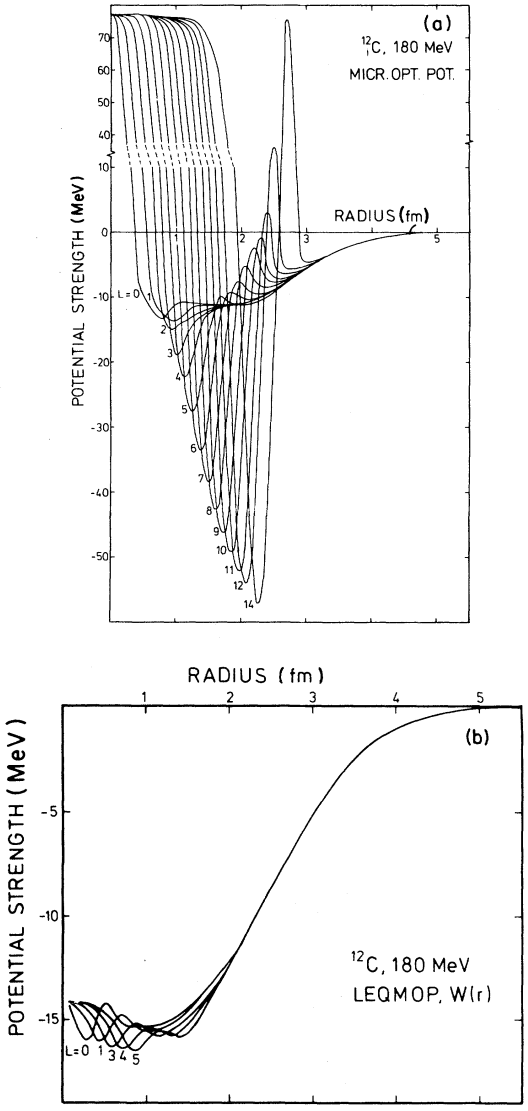

FIG. 14. (a) 180 MeV l-dependent real central potentials underlying the calculations in Fig. 12. (b) 180 MeV l-dependent imaginary central potentials underlying the calculations in Fig. 12.

form $L(L+1)$ for the real part. The imaginary part depends much less on the angular momentum. It has recently been shown[18] that such an angular momentum dependent potential can be phase equivalent to a normal energy-dependent potential of Woods-Saxon shape. This demonstrates the nonuniqueness of phase-equivalent potentials as stressed already in Sec. II. So the unusual shape of the local optical potential does not indicate that the phase shifts calculated from it are different from those for a more conventional potential. The reason for these oscillations which were not found in the Frahn-Lemmer case seems to be the strong repulsive odd state force. It enters into direct and exchange parts with opposite sign. If it were of zero range it would cancel out completely. Because of its infinite (though short) range some contribution from it remains in the final potential leading to the oscillatory behavior. So the oscillations do not seem to be peculiar to a density-dependent t matrix, but seem to be related to the strength of the odd state force in the underlying NN interaction.

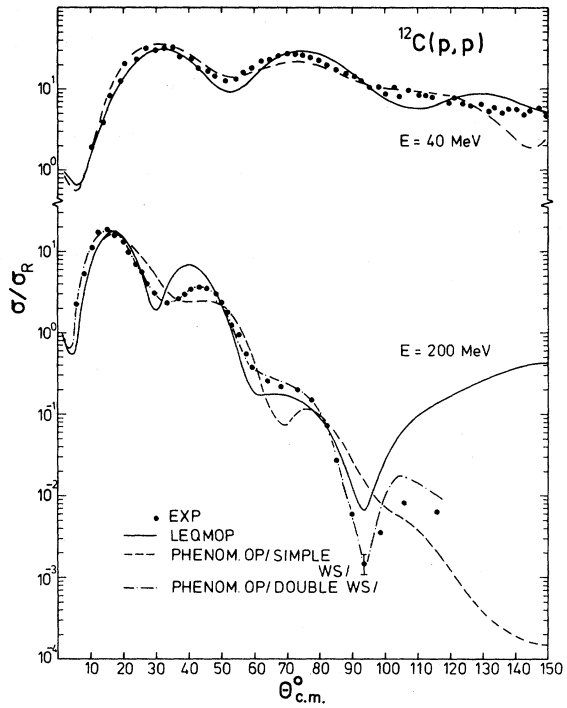

FIG. 15. ^{12}C proton scattering analyses for two energies. The data are from the literature (Refs. 19 and 20). Phenomenological OMP are the best fit potentials of Ref. 20 with single and double Saxon-Woods form factors.

For completeness we add in Figs. 11(a)–11(c) the numerical results for the imaginary and spin orbit potentials together with the damping function for $L=0$. In fact, all these quantities are l dependent. We will not discuss these terms further due to their minor importance or small physical significance in interpreting results.

IV. APPLICATIONS

Microscopic optical potentials have been shown to reproduce the global features of phenomenological results. Among these are the energy dependence of volume integrals of real and imaginary central potentials, the rms radii and in some cases (with adjustments of the strength by 10–20%) the reproduction of differential cross sections and polarizations. With the analysis presented here we do not expect to achieve better agreement but rather indicate characteristics which are inherent in nonlocal potentials.

The energy dependence of (equivalent) local potentials is well known as is the damping of nonlocal wave functions. The success of Saxon-Woods potentials below 80 MeV on the other hand indicates that the inner region of the target nucleus does not have a significant influence on angular distributions. Inclusion of the l-dependent core must therefore leave calculated angular distributions unaltered for low energies. In Figs. 12–14 proton scattering from ^{12}C is displayed for 40 and 180 MeV. The angular distributions are calculated with the full phase equivalent microscopic OMP (LEQ MOP) with and without spin orbit potentials ($U_{so}=0$). The second group of curves is obtained when the potential is replaced by the microscopic potential for $L=0$ and its core eliminated (LEQ MOP without core). The results show that the core is important only for high energies and large momentum transfers. In this kinematic region its effects are comparable to those of a spin-orbit potential. In Figs. 15 and 16 we compare the results with experimental data. The angular momentum dependent microscopic potential has been calculated up to a maximum angular momentum L_{max}, and the potential for L_{max} was

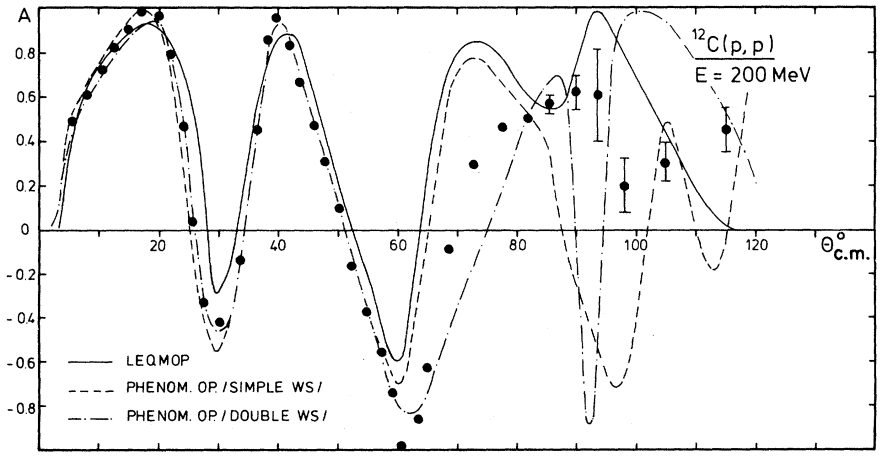

FIG. 16. Polarization for the 200 MeV analyses in Fig. 15.

used for all higher partial waves. L_{max} has been determined so that increasing it further does not change the angular distribution appreciably. Its value depends on the target nucleus and the bombarding energy. For ^{12}C and 180 MeV, a value of $L_{max}=12$ has been found if stability up to extreme backwards angles is required. For forward angles only (i.e., up to 90°), a smaller value around $L_{max}=5$ is sufficient. This reflects the greater sensitivity of large angle data to the form of the potential inside the target nucleus. The value for L_{max} gives an indication on the number of partial waves which feel the influence of the core. Since LEQ MOP represents an *ab initio* calculation its fit is excellent also compared to phenomenological fits. The 200 MeV data give reason to believe that large angle scattering is most strongly influenced by the core. The minimum in $\sigma(\theta)$ around 95° is followed by a backward rise. Similar results are obtained for 160 and 180 MeV scattering from ^{40}Ca, Figs. 17 and 18. Again we emphasize the rise after the minimum around 98°. The forward region is well reproduced with a

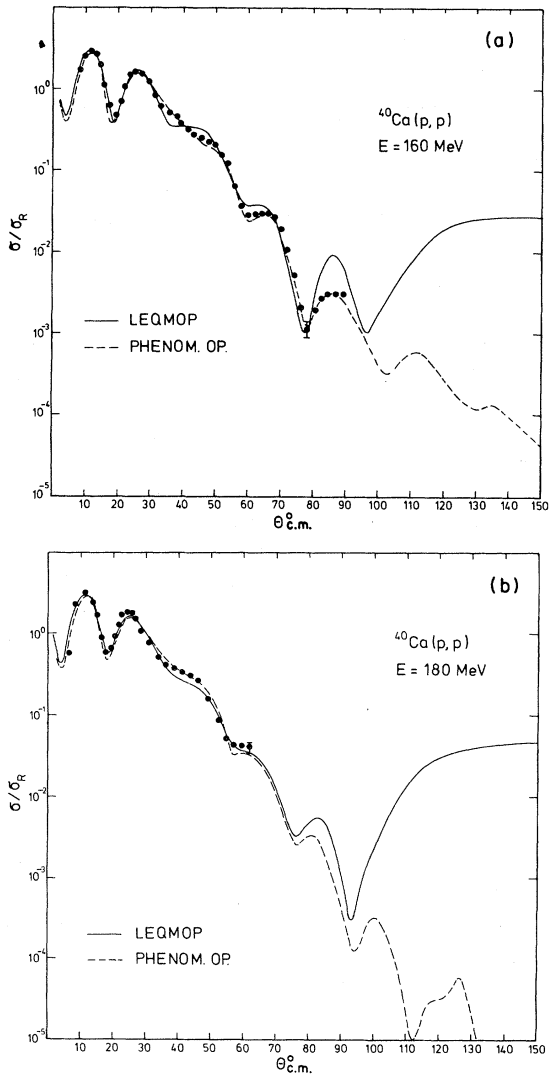

FIG. 17. (a) Comparison of 160 MeV proton scattering data with theoretical prediction with the LEQ. Experimental results are from Ref. 21. (b) Comparison of 180 MeV proton scattering data with theoretical prediction with the LEQ. Experimental results are from Ref. 21.

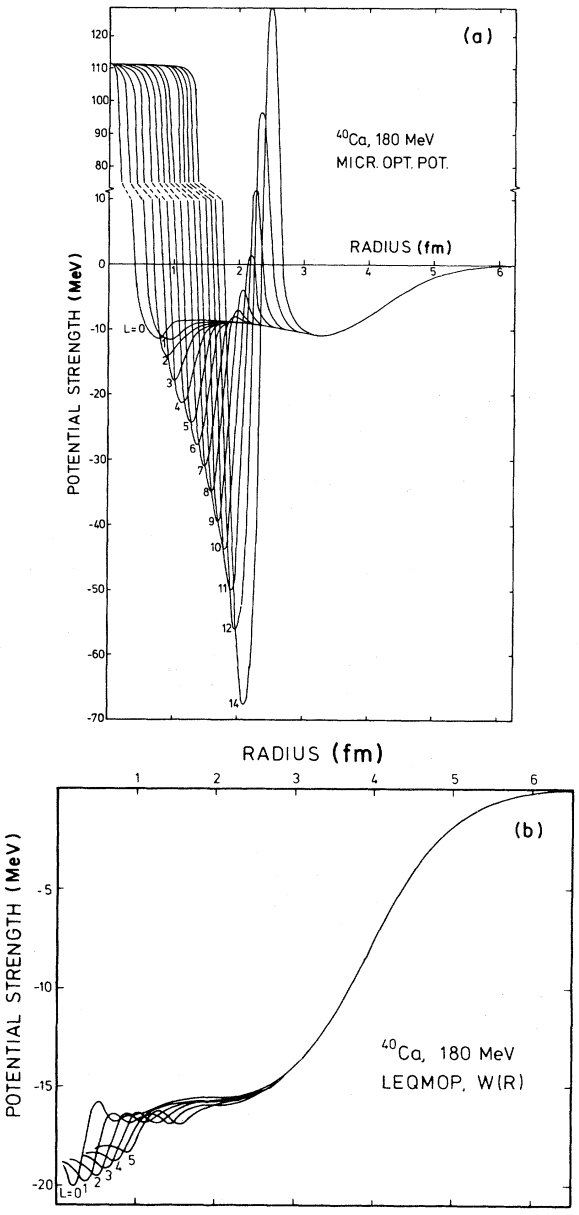

FIG. 18. (a) 180 MeV l-dependent real central potential underlying the calculations in Fig. 17(b). (b) 180 MeV l-dependent imaginary central potential underlying the calculations in Fig. 17(b).

strongly damped diffraction pattern between 30° and 70°. In phenomenological analyses this damping was explained as a pure spin orbit effect. A strong imaginary spin orbit potential is needed to reproduce this damping in a conventional Woods-Saxon parametrization. Such a potential is not found in theoretical approaches. We interpret the damping rather as a result of the effective l-dependent core together with the spin orbit potential. Every partial wave scatters from a different potential leading to a randomization effect which in turn results in a flat angular distribution.

In view of the underlying "10% theory" it is not our intention to overestimate the predictive power of microscopic OMP and their fits. The exact form of the backangle rise, e.g., depends on the detailed form of the density distribution of the target for small distances and also on the form of the optical potential close to the origin. These quantities may not be represented well enough by our approximations. So the actual form of the backangle cross section is not well established. Experiments have shown in the meantime that it is overestimated by the calculation.[22]

The damping of the diffraction pattern, on the other hand, is well established experimentally. In the energy region between 100 and 300 MeV, protons penetrate most deeply into the nucleus. So only for these energies are they sensitive to the form of the potential in the interior, i.e., to the angular momentum dependent core. Correspondingly, a large imaginary spin-orbit potential is needed only in this energy range to fit the data in conventional models. So we conclude that the large imaginary spin-orbit potential is only a phenomenological parametrization of the angular momentum dependent core in the real central potential. For these reasons, it is proposed that the analyses of future medium energy data be performed with nonlocal potentials which are either fully microscopic or at least guided by the microscopic treatment, like the phenomenological Frahn-Lemmer ansatz—which is convenient to handle in its multipole decomposition and contains fewer free parameters than superpositions of several local Woods-Saxon potentials.

This work was supported by the German Bundesministerium für Forschung und Technologie 06HH726.

---

*Present address: School of Physics, University of Melbourne, Parkville, Victoria, 3052, Australia.

†Present and permanent address: Central Research Institute for Physics, Budapest, Hungary.

[1] *Microscopic Optical Model Potential,* Lecture Notes in Physics, 89, edited by H. V. von Geramb (Springer, Berlin, 1979).

[2] J. P. Jeukenne, A. Lejeune, and C. Mahaux, Phys. Rep. 25C, 83 (1976).

[3] F. A. Brieva and J. R. Rook, Nucl. Phys. A291, 299 (1977); A291, 317 (1977); A297, 206 (1978).

[4] J. W. Negele and D. Vautherin, Phys. Rev. C 5, 1472 (1972); 11, 1031 (1975); X. Campi and A. Bouyssy, Phys. Lett. 73B, 263 (1978); A. Tielens, thesis, University of Hamburg, 1979 (unpublished).

[5] F. G. Perey and B. Buck, Nucl. Phys. 32, 353 (1962).

[6] W. E. Frahn and R. H. Lemmer, Nuovo Cimento 5, 523 (1957); 6, 664 (1957).

[7] F. G. Perey and D. S. Saxon, Phys. Lett. 10, 107 (1964); W. E. Frahn, Nucl. Phys. 66, 358 (1965); R. Peierls and N. VinhMau, Nucl. Phys. A343, 1 (1980); H. Horiuchi, Prog. Theor. Phys. 64, 184 (1980).

[8] N. Austern, Phys. Rev. 137, B752 (1965).

[9] H. Fiedeldey, Nucl. Phys. 77, 149 (1966); A96, 463 (1967); A115, 97 (1968).

[10] M. Coz, L. G. Arnold, and A. D. MacKellar, Ann. Phys. (N.Y.) 58, 504 (1970); 59, 219 (1970).

[11] F. G. Perey, in *Proceedings of the Conference on Direct Interactions and Nuclear Reaction Mechanisms, Padova, 1963,* edited by E. Clementel and C. Villi (Gordon and Breach, New York, 1963), p. 125.

[12] N. VinhMau and A. Bouyssy, Nucl. Phys. A257, 189 (1976).

[13] M. K. Weigel and G. Wegmann, Fortschr. Phys. 19, 451 (1971).

[14] T. Ueberall, thesis, University of Hamburg, 1979 (unpublished).

[15] L. G. Arnold and A. D. MacKellar, Phys. Rev. C 3, 1095 (1971); Th. O. Krause and B. Mulligan, Ann. Phys. (N.Y.) 94, 31 (1975); B. Mulligan, L. G. Arnold, B. Badchi, and Th. O. Krause, Phys. Rev. C 13, 2131 (1976).

[16] F. Capuzzi, Nuovo Cimento 11A, 801 (1972).

[17] B. Giraud and B. Grammaticos, Ann. Phys. (N.Y.) 101, 670 (1976).

[18] W. Bauhoff, Phys. Rev. C 27, 1822 (1983).

[19] B. W. Riedley and J. F. Turner, Nucl. Phys. 58, 497 (1964).

[20] H. O. Meyer, P. Schwandt, G. L. Moake, and P. P. Singh, Phys. Rev. C 23, 616 (1981).

[21] A. Nadasen, P. Schwandt, P. P. Singh, W. W. Jacobs, A. D. Bacher, P. T. Debecev, M. D. Kaitchuk, and J. T. Meek, Phys. Rev. C 23, 1023 (1981).

[22] H. O. Meyer, J. Hall, W. W. Jacobs, P. Schwandt, and P. P. Singh, Phys. Rev. C 24, 1782 (1981).